

Landau gauge ghost and gluon propagators in $SU(2)$ lattice gauge theory: Gribov ambiguity revisited

I.L. Bogolubsky

Joint Institute for Nuclear Research, 141980 Dubna, Russia

G. Burgio and M. Müller-Preussker

Humboldt-Universität zu Berlin, Institut für Physik, 12489 Berlin, Germany

V.K. Mitrjushkin

*Joint Institute for Nuclear Research, 141980 Dubna, Russia and
Institute of Theoretical and Experimental Physics, Moscow, Russia*

(Dated: November 23, 2005)

We reinvestigate the problem of Gribov ambiguities within the Landau (or Lorentz) gauge for the ghost and gluon propagators in pure $SU(2)$ lattice gauge theory. We make use of the full symmetry group of the action taking into account *large*, i.e. non-periodic global $\mathbb{Z}(2)$ gauge transformations leaving lattice plaquettes invariant. Enlarging in this way the gauge orbits for any given gauge field configuration the Landau gauge can be fixed at higher local extrema of the gauge functional in comparison with standard (overrelaxation) techniques. This has a clearly visible effect not only for the ghost propagator at small momenta but also for the gluon propagator, in contrast to previous observations.

PACS numbers: 11.15.Ha, 12.38.Gc, 12.38.Aw

Keywords: Landau gauge, Gribov problem, gluon propagator, ghost propagator

I. INTRODUCTION

It is an important task to compute (Landau or Coulomb) gauge gluon, ghost, fermion propagators and the basic vertex functions from non-perturbative approaches to $SU(N)$ gauge theories, like Dyson-Schwinger equations or the lattice. On one hand one is interested in their behaviour in the infrared limit in order to extract non-perturbative informations on various observables, e.g. the QCD running couplings $\alpha_s(q^2)$, to understand quark and gluon confinement within the Gribov-Zwanziger scenario [1, 2, 3], or to check the Kugo-Ojima confinement criterion for the absence of colored states [4]. On the other hand it is technically important to see to what extent these different non-perturbative approaches provide results consistent with each other in the non-perturbative region, i.e. at low momenta. At present we are still far from drawing final conclusions in this respect. In particular the Dyson-Schwinger approach [5, 6, 7], always relying on a truncated set of equations, provides results which look quite different in the infinite volume limit compared with those obtained on a torus [8, 9, 10], while the latter show at least qualitative agreement with recent results of numerical lattice simulations [11].

It is well known that gauge fixing in the non-

perturbative range is faced with the Gribov ambiguity problem, which means that there can be many gauge copies for a given gauge field satisfying the Landau gauge condition $\partial_\mu A_\mu = 0$ within the Gribov region, the latter defined by the positivity of the Landau gauge Faddeev-Popov operator. In recent years one has checked in greater detail how strong Gribov copies can influence the infrared behavior especially of the gluon and ghost propagators. Several groups of authors [11, 12, 13, 14] came to the conclusion that while there is a visible influence on the ghost propagator, the gluon propagator seems only very weakly affected within the statistical (Gribov) noise.

Recently Zwanziger has argued that in the infinite volume limit the influence of Gribov copies should be negligible, i.e. all copies within the Gribov region should become equivalent [3]. However in practical lattice simulations we are always restricted to finite volumes. Thus, Gribov copies have to be taken into account properly before extrapolating to the infrared and infinite volume.

In this paper we present a reinvestigation of the Gribov copy problem for the $SU(2)$ case. The usual way to fix the (Landau) gauge on the lattice is to simulate the path integral in its gauge invariant form. Subsequently each of the produced lattice gauge fields $U \equiv \{U_{x,\mu}\}$ is subjected

to an iterative procedure maximizing the gauge functional

$$F(g) = \frac{1}{dV} \sum_{x,\mu} \frac{1}{2} \text{Tr } U_{x,\mu}^g, \quad (1)$$

$$U_{x,\mu}^g = g(x) U_{x,\mu} g^\dagger(x + \hat{\mu})$$

with respect to local gauge transformations $g \equiv \{g(x) \in SU(2)\}$. $V = L^d$ denotes the number of lattice sites in $d = 4$ dimensions. The local maxima of $F(g)$ satisfy the differential lattice Landau gauge transversality condition

$$(\partial_\mu A_\mu^g)(x) = A_\mu^g(x + \hat{\mu}/2) - A_\mu^g(x - \hat{\mu}/2) = 0, \quad (2)$$

where the lattice gauge potentials are

$$A_\mu(x + \hat{\mu}/2) = \frac{1}{2i} (U_{x,\mu} - U_{x,\mu}^\dagger). \quad (3)$$

The standard procedure assumes *periodic gauge transformations* and employs the *overrelaxation algorithm*. In what follows we shall abbreviate it by *SOR*. The influence of Gribov copies can be easily studied by taking various initial random gauge copies of the gauge field configurations before subjecting them to the SOR algorithm. In Refs. [13] for $SU(2)$ and [11] for $SU(3)$ the impact of Gribov copies has been studied in a thorough manner within the SOR framework. As already mentioned the gluon propagator did not depend on the copies within the statistical noise, whereas the ghost propagator clearly depended on them in the infrared. But the data for the ghost propagator obtained for different lattice sizes showed an indication for a weakening of the dependence on the choice of Gribov copies for increasing lattice size at fixed momentum, in agreement with Zwanziger's claim [3].

Here we enlarge the class of possible gauge transformations by taking into account also *non-periodic* center gauge transformations. This will allow us to maximize further the gauge functional and to see a quite strong Gribov copy effect even for the gluon propagator at finite (lattice) volumes.

In Sec. II we shall explain the improved gauge fixing procedure. In Sec. III we define the propagators to be calculated. In Sec. IV we are going to present our results for the gluon and ghost propagators, whereas in Sec. V the conclusions will be drawn.

II. IMPROVED GAUGE FIXING

We shall deal all the time with $SU(2)$ pure gauge lattice fields in four Euclidean dimensions produced by means of Monte Carlo simulations with the standard Wilson plaquette action. We restrict ourselves to the confinement phase at $T = 0$.

To fix the gauge we employ the standard Los Alamos type overrelaxation with $\omega = 1.7$.

Our generalization of the standard gauge fixing procedure SOR comes from the simple observation that gauge covariance for periodic $SU(2)$ gauge fields on a d -dimensional torus of extension L^d allows gauge transformations which are not necessarily periodic but can differ by a group center element at the boundary:

$$g(x + L\hat{\nu}) = z_\nu g(x), \quad z_\nu = \pm 1 \in \mathbb{Z}(2). \quad (4)$$

In light of this it is legitimate to allow, during the maximization of the gauge functional in the gauge fixing procedure, for gauge transformations which differ by a sign when winding around a boundary. Let ν be the direction of such boundary. Any such gauge transformation can be decomposed into a standard periodic gauge transformation (which we may call a “small” one) and a flip of all links $U_\nu(x) \rightarrow -U_\nu(x)$ of a 3-plane at a given fixed x_ν . Given a “small” random gauge copy of the configuration we have thus performed a pre-conditioning step for the gauge functional by sweeping in every direction all 3-planes in succession and comparing the value of the flipped with the unflipped gauge functional. The flip is accepted if the gauge functional increases. It is easy to see that such a procedure is independent of the order of choosing the 3-planes and that only one sweep through the lattice is required to maximize the functional. The gauge copy obtained at the end of this procedure is then used as a starting point for a standard maximization procedure. We call the whole procedure FOR.

Analogously to the SOR method the FOR procedure can be repeated with different initial random gauges in order to find a best copy (**bc**) in comparison e.g. with the first random copy (**fc**). We shall check the convergence of the **bc**-propagator results for the best copies as a function of the number n_{copy} of random initial copies.

III. GLUON AND GHOST PROPAGATORS

We turn now to the computation of the gauge variant gluon and ghost propagators within the Landau gauge.

The lattice gluon propagator $D_{\mu\nu}^{ab}(p)$ is taken as the Fourier transform of the gluon two-point function, *i.e.* the expectation value

$$\begin{aligned} D_{\mu\nu}^{ab}(p) &= \left\langle \tilde{A}_\mu^a(\hat{k}) \tilde{A}_\nu^b(-\hat{k}) \right\rangle_U \\ &= \delta^{ab} \left(\delta_{\mu\nu} - \frac{p_\mu p_\nu}{p^2} \right) D(p). \end{aligned} \quad (5)$$

$\tilde{A}_\mu^a(\hat{k})$ is the Fourier transform of the lattice gauge potential $A_\mu^a(x + \hat{\mu}/2)$. p denotes the four-momentum

$$p_\mu(\hat{k}_\mu) = \frac{2}{a} \sin \left(\frac{\pi \hat{k}_\mu}{L} \right) \quad (6)$$

with the integer-valued lattice momentum $\hat{k}_\mu \in (-L/2, +L/2]$. a is the lattice spacing.

The lattice ghost propagator is defined by inverting the Faddeev-Popov (F-P) operator, the latter being the Hessian of the gauge functional Eq. (1). The F-P operator can be written in terms of the (gauge-fixed) link variables $U_{x,\mu}$ as

$$M_{xy}^{ab} = \sum_\mu A_{x,\mu}^{ab} \delta_{x,y} - B_{x,\mu}^{ab} \delta_{x+\hat{\mu},y} - C_{x,\mu}^{ab} \delta_{x-\hat{\mu},y} \quad (7)$$

with

$$\begin{aligned} A_{x,\mu}^{ab} &= \frac{1}{2} \delta_{ab} \text{Tr} [U_{x,\mu} + U_{x-\hat{\mu},\mu}], \\ B_{x,\mu}^{ab} &= \frac{1}{2} \Re \text{Tr} [\sigma^b \sigma^a U_{x,\mu}], \\ C_{x,\mu}^{ab} &= \frac{1}{2} \Re \text{Tr} [\sigma^a \sigma^b U_{x-\hat{\mu},\mu}], \end{aligned}$$

where the σ^a , $a = 1, 2, 3$ are the Pauli matrices. In the continuum M_{xy}^{ab} corresponds to the operator $M^{ab} = -\partial_\mu D_\mu^{ab}$, with D^{ab} the covariant derivative in the adjoint representation.

The ghost propagator in momentum space is calculated from the ensemble average

$$G^{ab}(p) = \frac{1}{V} \sum_{x,y} \left\langle e^{-2\pi i \hat{k} \cdot (x-y)} [M^{-1}]_{xy}^{ab} \right\rangle_U \quad (8)$$

$$= \delta^{ab} G(p). \quad (9)$$

Following Ref. [12, 15] we have used the conjugate gradient (CG) algorithm to invert M on a plane wave $\vec{\psi}_c = \{ \delta_{ac} \exp(2\pi i \hat{k} \cdot x) \}$.

After solving $M\vec{\phi} = \vec{\psi}_c$ the resulting vector $\vec{\phi}$ is projected back on $\vec{\psi}$ so that the average $G^{cc}(p)$ over the color index c can be taken explicitly. Since the F-P operator M is zero if acting on constant modes, only $\hat{k} \neq (0, 0, 0, 0)$ is permitted. Due to high computational requirements to invert the F-P operator for each \hat{k} , separately, the estimators on a single, gauge-fixed configuration are evaluated only for a preselected set of momenta \hat{k} .

IV. RESULTS

We consider various bare couplings in the interval $\beta = 4/g_0^2 \in [2.1, 2.5]$ and lattice sizes up to 20^4 . We compare the gluon and ghost propagators obtained with the alternative gauge fixing methods SOR ('flips off') and FOR ('flips on') both for the first (fc) and best copy (bc). In order to find the best copies we always generate 20 initial random gauge copies.

In Fig. 1 we illustrate for the FOR method how fast the gluon and ghost propagators are converging when determined from the best copy out of the first n_{copy} copies. We see plateaus occurring for $n_{copy} \geq O(10)$. We have convinced ourselves that $O(20)$ copies are sufficient at least for $\beta \geq 2.3$ and lattice sizes up to 20^4 . Mostly we have concentrated on the lowest non-trivial on-axis lattice momentum $p_{min} = (2/a) \sin(\pi/L)$ and some multiple on-axis momenta in order to study the infrared limit for given lattice size and bare coupling. We are aware of the fact that this choice is by far too restrictive in order to get reliable results for the (renormalized) propagators in the continuum and thermodynamic limit.

In Fig. 2 and Fig. 3 we show our results for the lattice gluon $D(p_{min})$ and ghost propagators $G(p_{min})$ for 12^4 and 16^4 lattices, always for the smallest non-vanishing momentum. In order to demonstrate the effect of the $\mathbb{Z}(2)$ flips in comparison with the SOR results obtained with bc and fc copies [13] we show three sets of data points: black dots correspond to FOR - 'flips on' and bc copies and open circles (squares) correspond to SOR - 'flips off' for bc (fc) copies. The corresponding data are listed in Table I.

We clearly see that the FOR method leads to an additional visible Gribov copy effect not

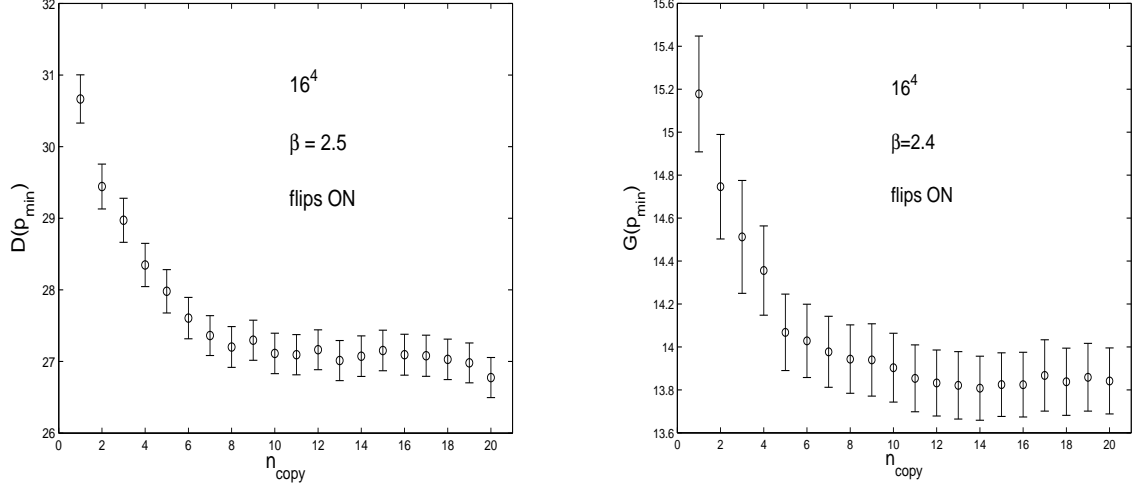


FIG. 1: Gluon propagator (left) and ghost propagator (right) at lowest momentum $p_{min} = (2/a)\sin(\pi/L)$ versus number of random copies employing the FOR method ('flips on') at $\beta = 2.5$ and 2.4 , respectively (lattice size 16^4).

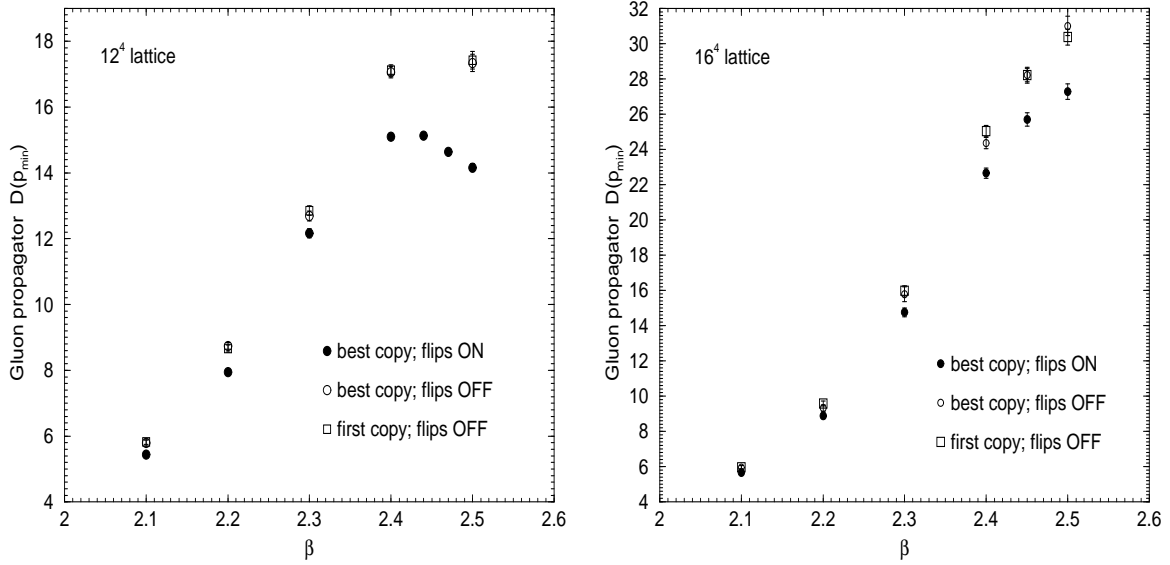
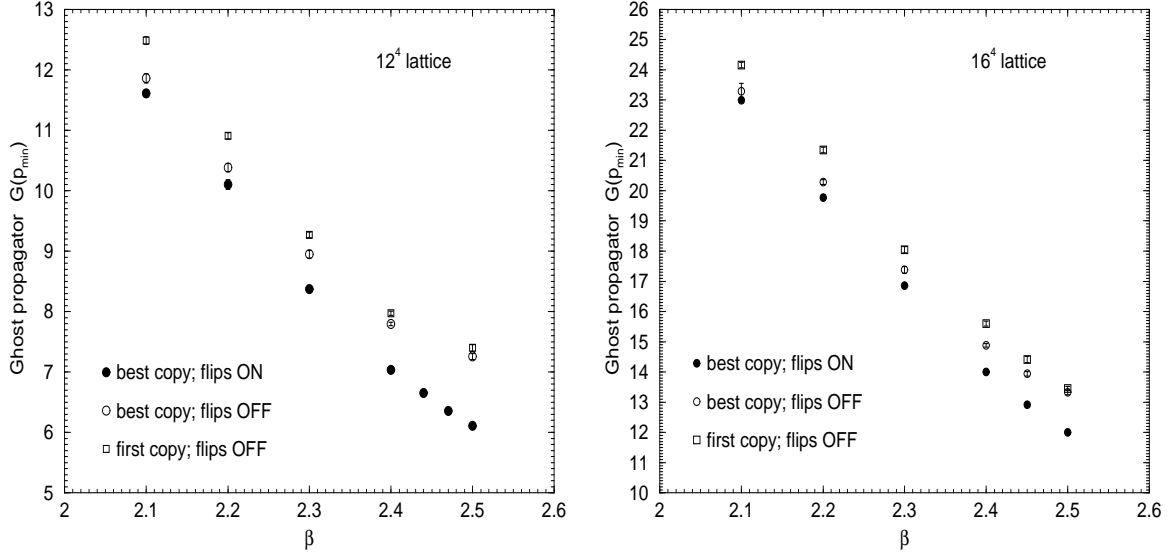


FIG. 2: Gluon propagator $D(p_{min})$ at lowest momentum for various β and for lattice sizes 12^4 (left) and 16^4 (right). Full dots refer to FOR **fc** and open squares (circles) correspond to SOR **fc** (**bc**).

only for the ghost propagator but also for the gluon propagator in contrast to the common claim based on purely periodic gauge transformations. The effect is even more pronounced at higher β -values.

In order to illustrate the strong Gribov copy effect in a slightly different manner we compare

smoothed distributions for the mean value estimators for the gluon and ghost propagators for the **bc** with the FOR and SOR method, respectively (see Fig. 4). The mean value distributions have been obtained in accordance with the bootstrap method [16] from replica of sequences of randomly selected data. Such bootstrapped resampling was applied to the initial

FIG. 3: Ghost propagator $G(p_{min})$ as for Fig. 2.

12^4					
β	#	$D_{\text{FOR}}^{(bc)}$	#	$D_{\text{SOR}}^{(bc)}$	$D_{\text{SOR}}^{(fc)}$
2.10	1200	5.39(6)	900	5.79(8)	5.83(8)
2.20	1200	7.94(9)	1200	8.74(10)	8.66(10)
2.30	1200	12.16(14)	1200	12.69(15)	12.85(15)
2.40	3600	15.10(10)	2080	17.06(17)	17.12(17)
2.44	5100	15.13(9)			
2.47	5700	14.64(9)			
2.50	2650	14.16(13)	1760	17.34(26)	17.42(26)

16^4					
β	#	$D_{\text{FOR}}^{(bc)}$	#	$D_{\text{SOR}}^{(bc)}$	$D_{\text{SOR}}^{(fc)}$
2.10	1042	5.59(7)	918	5.93(8)	5.95(8)
2.20	900	9.01(12)	740	9.35(14)	9.58(14)
2.30	1100	14.88(18)	510	16.16(31)	15.97(29)
2.40	1032	22.65(29)	1020	24.36(32)	25.03(32)
2.45	1020	25.69(32)	1030	28.19(36)	28.21(38)
2.50	1040	26.86(35)	1060	30.64(44)	30.37(45)

12^4					
β	#	$G_{\text{FOR}}^{(bc)}$	#	$G_{\text{SOR}}^{(bc)}$	$G_{\text{SOR}}^{(fc)}$
2.10	1200	11.58(4)	900	11.87(4)	12.48(7)
2.20	1200	10.10(8)	1200	10.39(3)	10.90(5)
2.30	1200	8.37(2)	1200	8.99(6)	9.27(4)
2.40	3600	7.04(1)	2080	7.80(3)	7.97(4)
2.44	5100	6.65(1)			
2.47	5700	6.36(1)			
2.50	2650	6.11(1)	1760	7.26(5)	7.40(5)

16^4					
β	#	$G_{\text{FOR}}^{(bc)}$	#	$G_{\text{SOR}}^{(bc)}$	$G_{\text{SOR}}^{(fc)}$
2.10	1042	22.89(6)	918	23.12(13)	24.15(8)
2.20	900	19.83(6)	740	20.29(6)	21.34(9)
2.30	1100	16.83(5)	510	17.27(8)	18.05(10)
2.40	1032	14.00(4)	1020	14.88(6)	15.60(8)
2.45	1020	12.92(5)	1030	13.86(6)	14.41(11)
2.50	1040	12.02(4)	1060	13.26(6)	13.45(7)

TABLE I: Data for the gluon propagator $D(p)$ (left) as well as for the ghost propagator $G(p)$ (right) at lowest momentum $p = p_{min}$ obtained with FOR (bc) and SOR (bc and fc) methods on 12^4 and 16^4 lattices.

MC data set as a whole, the amount of replicas being typically 200. To smoothen the distribution we have used the standard Nadaraya–Watson method with normal kernel [17], and an improved Silverman’s rule of thumb for the choice of the corresponding bandwidth.

It is worth mentioning that the statistical errors for most of our data have also been estimated through bootstrapped resampling.

We have also studied how the Gribov copy effect develops for larger momenta $p(\hat{k})$. We have used multiples of the minimal lattice momentum

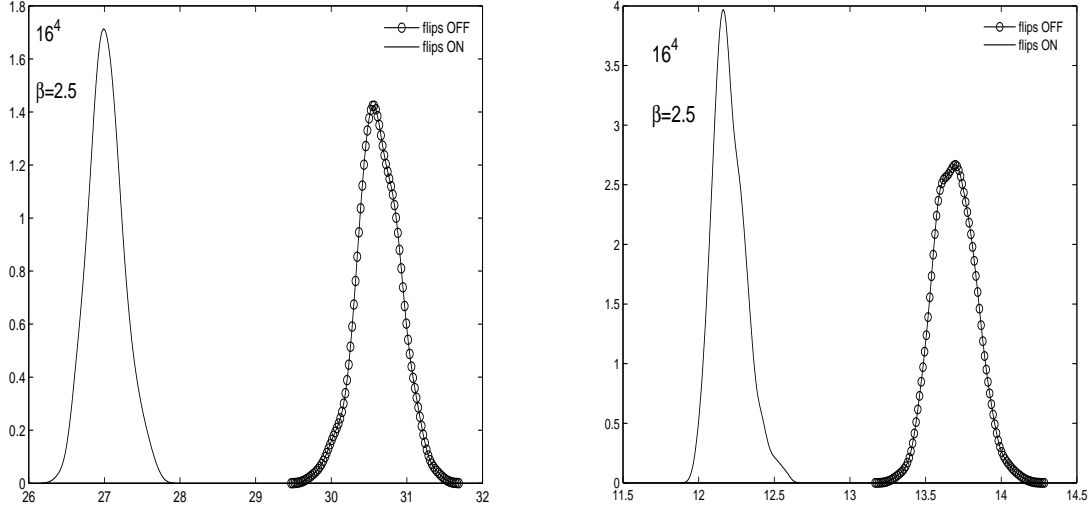


FIG. 4: SOR- and FOR-distributions for $D^{(bc)}(p_{min})$ (left) and $G^{(bc)}(p_{min})$ (right) at $\beta = 2.5$ and 16^4 lattice.

$\hat{k} = (0, 0, 0, k)$, $k = 1, 2, 3, 4$ along one axis. We compare for the gluon propagator the **bc** SOR results with **bc** FOR results in terms of the relative deviation

$$\delta D(p) = (D_{\text{SOR}}^{(bc)} - D_{\text{FOR}}^{(bc)})/D_{\text{FOR}}^{(bc)}, \quad (10)$$

and analogously for the ghost propagator $G(p)$ at various β -values and with fixed lattice size 16^4 (see Fig. 5). For the gluon propagator our results are restricted to only one β -value because of the much stronger statistical noise. Nevertheless, the results presented for the gluon propagator point into the same direction as for the ghost propagator. The effect of Gribov copies still remains noticeable at $p > p_{min}$, although decreasing for rising momenta.

The data for the ghost propagator at various momenta obtained from independent Monte Carlo runs are also collected in Table II.

It is interesting to study the volume dependence of the Gribov copy effect, in view of Zwanziger's recent claim mentioned at the beginning [3]. For this we have plotted in Fig. 6 the relative deviation

$$\delta D_L(p_{min}) \equiv (D_{\text{SOR}}^{(fc)} - D_{\text{FOR}}^{(bc)})/D_{\text{FOR}}^{(bc)} \quad (11)$$

for the gluon propagator and analogously for the ghost propagator as a function of the inverse linear lattice size $1/L$, both determined at the minimal momentum p_{min} . Here we have used

data for fixed $\beta = 2.4$ and lattice sizes from $L = 5$ up to $L = 20$. We see that the Gribov copy effect becomes weaker for increasing lattice size and correspondingly decreasing minimal momentum, at least up to a certain value of the lattice size ($\lesssim 15$). One would of course need larger values of L to make a reliable conclusion about the limit $L \rightarrow \infty$. Anyway, at our largest lattice value $L = 20$ the Gribov copy effect is still strong.

For the ghost propagator, where the signal to noise ratio is more favourable, we have found an analogous behavior also for the multiple on-axis momenta $k = 2, 3, 4$ (see Fig. 7).

In [13] two of us have reported on rare Monte Carlo events with exceptionally large values of the ghost propagator occurring for the SOR gauge fixing method for larger β values. In Fig. 8 we show some time histories for the gluon and ghost propagators for $\beta = 2.5$ and a 16^4 lattice, comparing **bc** SOR with **bc** FOR. We see that for the 'best copy - flips on' case (FOR) the fluctuations for both propagators are smaller. But for the ghost propagator the effect of exceptionally large values, in general related to small eigenvalues of the F-P operator [18], is still there.

Concluding we show the form factors of the gluon propagator $p^2 D(p)$ and of the ghost propagator $p^2 G(p)$ in physical units as a function of the physical momentum for fixed $\beta = 2.4$ and lattice sizes varying from 10^4 to 20^4 . We have

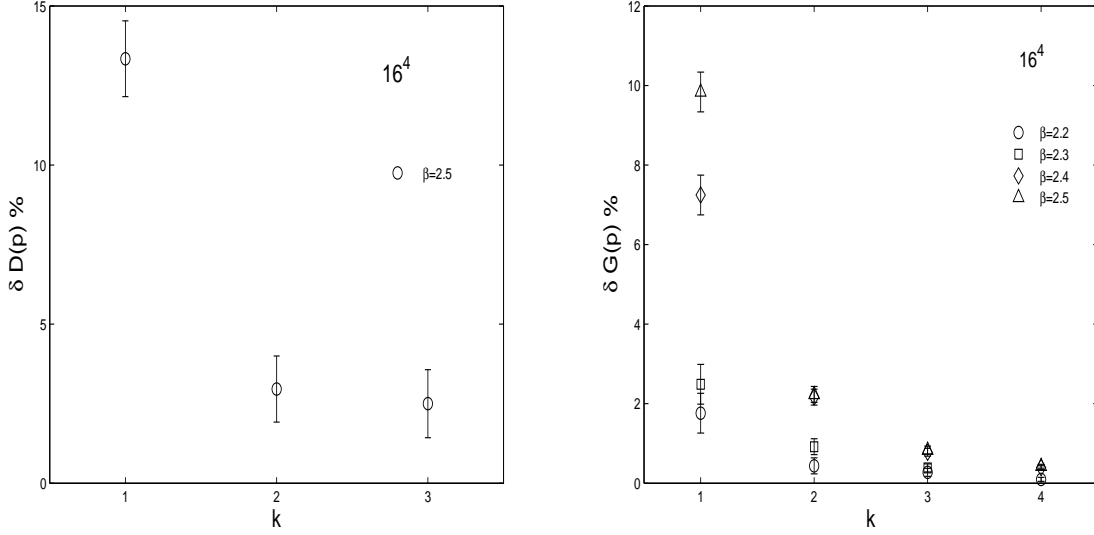


FIG. 5: Left: relative deviation $\delta D(p) = (D_{\text{SOR}}^{(bc)} - D_{\text{FOR}}^{(bc)})/D_{\text{FOR}}^{(bc)}$ in percent for the gluon propagator at various (on-axis) lattice momenta $p(k)$ (lattice size 16^4 , $\beta = 2.5$). Right: the analogous relative deviation for the ghost propagator for the same lattice size but for $\beta = 2.2, 2.3, 2.4$ and 2.5 .

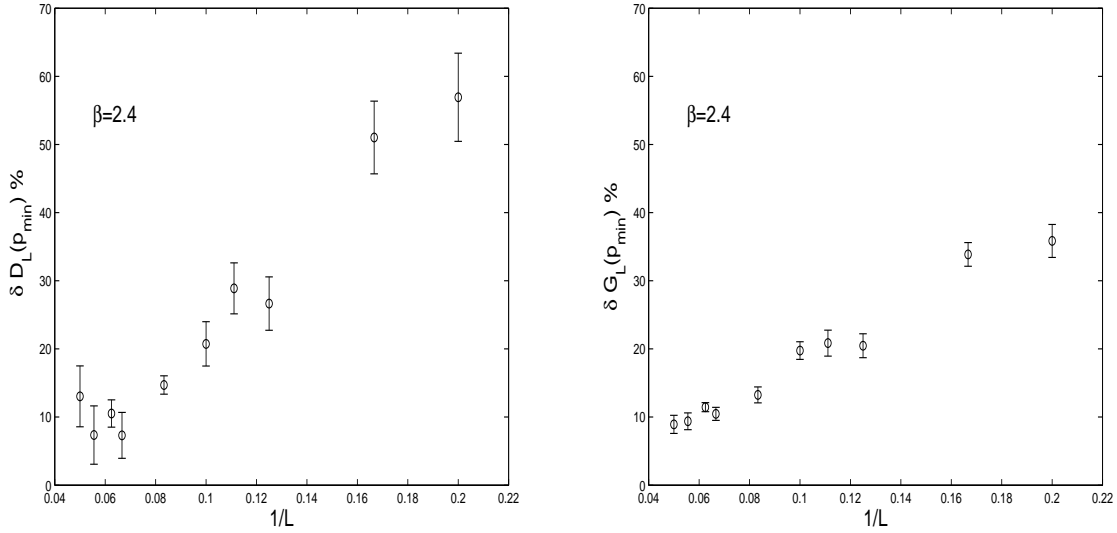


FIG. 6: Relative deviation $\delta D_L(p_{\min}) \equiv (D_{\text{SOR}}^{(fc)} - D_{\text{FOR}}^{(bc)})/D_{\text{FOR}}^{(bc)}$ in percent for the gluon propagator D (left) and analogously for the ghost propagator G (right) for various linear lattice sizes L , always determined for the smallest non-vanishing momentum $p_{\min} = (2/a)\sin(\pi/L)$ ($\beta = 2.4$).

rescaled the gluon propagator values $D(p)$ with factors a^2 and g_0^2 and the ghost propagator $G(p)$ with a^2 , respectively, in order to translate to the corresponding continuum (bare) propaga-

tors (compare with [19]). To estimate the lattice spacing in physical units we have used the string tension: $a^2\sigma = .071$ [20] with the standard value $\sqrt{\sigma} = 440\text{MeV}$. The form factor results for both

FOR						
β	#		$G(k=1)$	$G(k=2)$	$G(k=3)$	$G(k=4)$
2.20	400	fc	21.2(1)	3.96(1)	1.510(2)	0.8116(5)
		bc	19.88(8)	3.868(7)	1.493(1)	0.8076(4)
2.30	400	fc	18.2(2)	3.39(3)	1.313(2)	0.7276(6)
		bc	16.88(8)	3.267(6)	1.299(1)	0.7241(4)
2.40	356	fc	15.4(1)	2.87(1)	1.171(1)	0.6693(3)
		bc	13.8(1)	2.770(8)	1.156(2)	0.6647(4)
2.50	400	fc	13.7(1)	2.578(5)	1.0897(8)	0.6357(2)
		bc	12.2(1)	2.508(5)	1.079(1)	0.6325(3)
SOR						
β	#		$G(k=1)$	$G(k=2)$	$G(k=3)$	$G(k=4)$
2.20	200	fc	21.2(2)	3.97(2)8	1.511(3)	0.8117(7)
		bc	20.23(12)	3.885(10)	1.4971(25)	0.8084(7)
2.30	200	fc	18.2(1)	3.35(1)	1.312(2)	0.7272(5)
		bc	17.3(1)	3.297(8)	1.304(1)	0.7253(5)
2.40	370	fc	15.6(1)	2.87(1)	1.171(1)	0.6690(3)
		bc	14.8(1)	2.83(1)	1.165(1)	0.6673(3)
2.50	200	fc	14.1(2)	2.586(8)	1.090(1)	0.6359(4)
		bc	13.4(1)	2.564(6)	1.088(1)	0.6352(3)

TABLE II: Ghost propagators $G(p)$ on the 16^4 lattice for various on-axis lattice momenta $p(k)$.

methods bc SOR and bc FOR are shown together in Fig. 9. Again the figure shows clear Gribov copy effects for both the propagators and not only for the ghost propagator. We did not apply any overall renormalization here. The statistics collected for these runs is listed in Table III.

FOR										
L	5	6	8	9	10	12	15	16	18	20
N_{conf}	1000	1000	800	600	600	500	400	356	200	200
SOR										
L	5	6	8	9	10	12	15	16	18	20
N_{conf}	1000	1000	800	500	500	400	400	370	100	100

TABLE III: Statistics for the measurements at different L and $\beta = 2.4$.

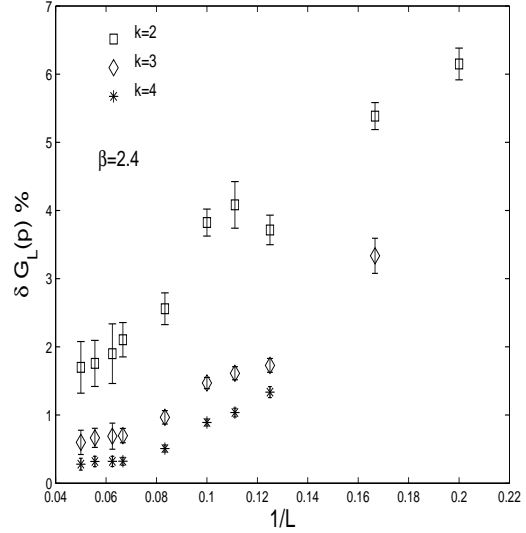


FIG. 7: As in Fig. 6 the relative deviation $\delta G_L(p) \equiv (G_{SOR}^{(fc)} - G_{FOR}^{(bc)})/G_{FOR}^{(bc)}$ in percent is shown for the ghost propagator G for various linear lattice sizes L and on-axis momenta $p(k)$, $k = 2, 3, 4$.

V. CONCLUSIONS

In this paper we have demonstrated that there is a visible Gribov problem for the ghost propagator as well as for the gluon propagator computed in $SU(2)$ lattice gauge theory within the Landau gauge. In order to show this we have enlarged the gauge orbits of given Monte Carlo generated gauge fields by non-periodic global $\mathbb{Z}(2)$ transformations, flipping all links in a given direction on a slice orthogonal to that. This allows a preconditioning which maximizes the gauge functional before applying the overrelaxation algorithm.

We have found indications for a weakening of the Gribov copy effect both going to larger momenta at fixed volume and also increasing the lattice size L while correspondingly lowering the minimal non-zero momentum, at least up to a certain value of the lattice size ($\lesssim 15$). However, one would need larger values of L to make any reliable conclusion about the limit $L \rightarrow \infty$.

We have not shown the momentum scheme running coupling which can be determined from the form factors of the propagators discussed here assuming that the renormalization factor for the ghost-gluon vertex is constant. This will be discussed in a future paper, where we want to

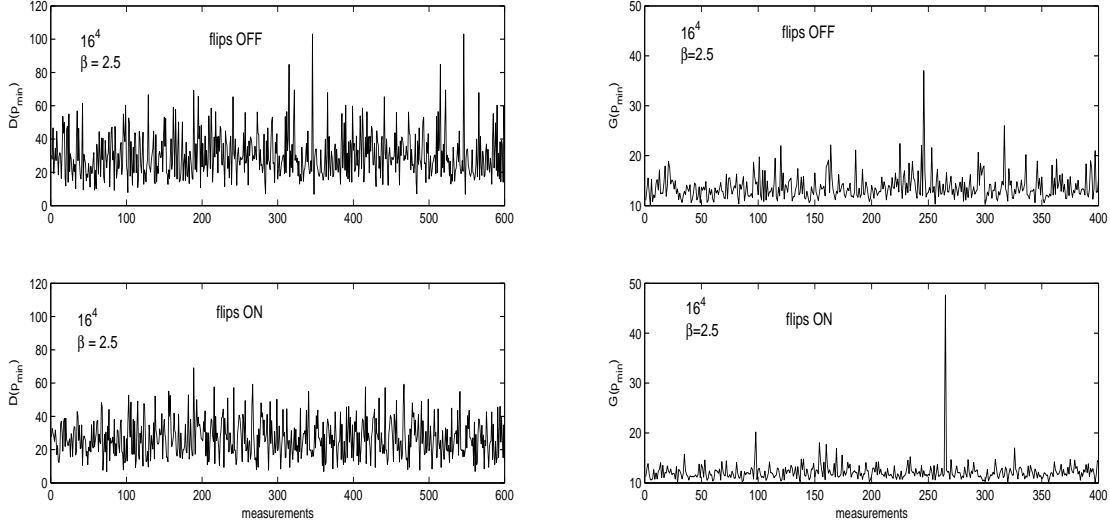


FIG. 8: Time histories for $D^{(bc)}(p_{min})$ (left) and $G^{(bc)}(p_{min})$ (right) for both SOR and FOR methods at $\beta = 2.5$ and 16^4 lattice.

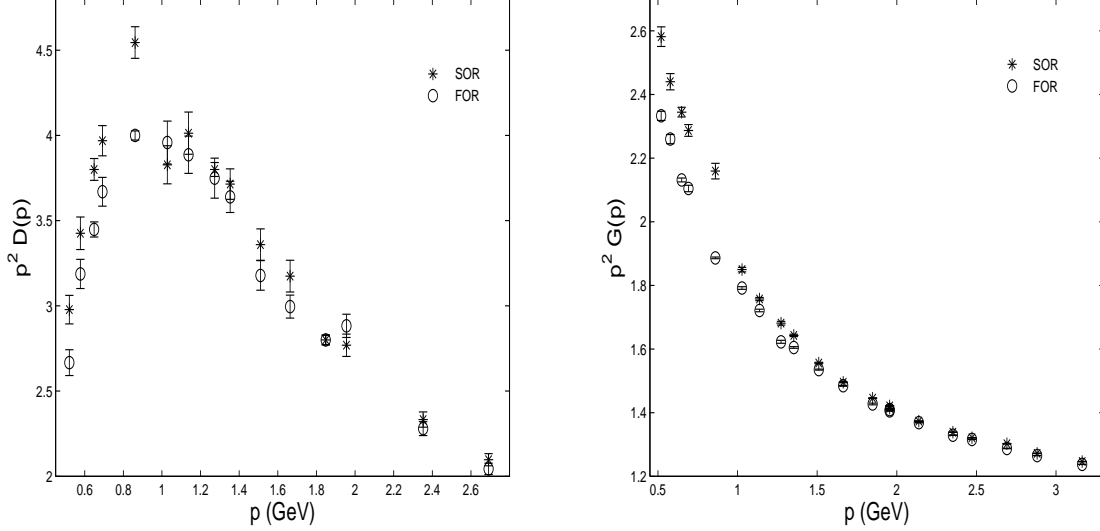


FIG. 9: Gluon form factor $p^2 D(p)$ (left) and ghost form factor $p^2 G(p)$ (right) both for the bc SOR and bc FOR methods versus momentum obtained for various lattice sizes and fixed $\beta = 2.4$.

present data for larger lattices and a larger spectrum of (off-axis) momenta.

ACKNOWLEDGEMENTS

This investigation has been supported by the Heisenberg-Landau program of collaboration between the Bogoliubov Lab of Theoretical Physics of the Joint Institute for Nuclear Research Dubna, Russia and german institutes. V.K.M.

acknowledges support by an RFBR grant 05-02-16306. G.B. acknowledges support from an INFN

fellowship. M.M.-P. thanks the DFG for support under grant FOR 465 / Mu932/2-2.

-
- [1] V. N. Gribov, Nucl. Phys. **B139**, 1 (1978).
 - [2] D. Zwanziger, Nucl. Phys. **B412**, 657 (1994).
 - [3] D. Zwanziger, Phys. Rev. **D69**, 016002 (2004), hep-ph/0303028.
 - [4] T. Kugo and I. Ojima, Prog. Theor. Phys. Suppl. **66**, 1 (1979).
 - [5] R. Alkofer and L. von Smekal, Phys. Rept. **353**, 281 (2001), hep-ph/0007355.
 - [6] C. S. Fischer and R. Alkofer, Phys. Rev. **D67**, 094020 (2003), hep-ph/0301094.
 - [7] C. Lerche and L. von Smekal, Phys. Rev. **D65**, 125006 (2002), hep-ph/0202194.
 - [8] C. S. Fischer, R. Alkofer, and H. Reinhardt, Phys. Rev. **D65**, 094008 (2002), hep-ph/0202195.
 - [9] C. S. Fischer and R. Alkofer, Phys. Lett. **B536**, 177 (2002), hep-ph/0202202.
 - [10] C. S. Fischer, B. Gruter, and R. Alkofer (2005), hep-ph/0506053.
 - [11] A. Sternbeck, E.-M. Ilgenfritz, M. Müller-Preussker, and A. Schiller, Phys. Rev. **D72**, 014507 (2005), hep-lat/0506007.
 - [12] A. Cucchieri, Nucl. Phys. **B508**, 353 (1997), hep-lat/9705005.
 - [13] T. D. Bakeev, E.-M. Ilgenfritz, V. K. Mitrushkin, and M. Müller-Preussker, Phys. Rev. **D69**, 074507 (2004), hep-lat/0311041.
 - [14] H. Nakajima and S. Furui, Nucl. Phys. Proc. Suppl. **129**, 730 (2004), hep-lat/0309165.
 - [15] H. Suman and K. Schilling, Phys. Lett. **B373**, 314 (1996), hep-lat/9512003.
 - [16] B. Efron and R. J. Tibshirani, *An introduction to the Bootstrap* (Chapman & Hall, 1993).
 - [17] A. W. Bowman and A. Azzalini, *Applied Smoothing Techniques for Data Analysis: the Kernel method* (Oxford University Press, 1997).
 - [18] A. Sternbeck, E. M. Ilgenfritz, and M. Mueller-Preussker (2005), hep-lat/0510109.
 - [19] J. C. R. Bloch, A. Cucchieri, K. Langfeld, and T. Mendes, Nucl. Phys. **B687**, 76 (2004), hep-lat/0312036.
 - [20] J. Fingberg, U. M. Heller, and F. Karsch, Nucl. Phys. **B392**, 493 (1993), hep-lat/9208012.